Acta Neuropathol (2004) 107 : 504–508
DOI 10.1007/s00401-004-0842-2

REGULAR PAPER

**Takashi Togo · Haruhiko Akiyama · Eizo Iseki
Hirotake Uchikado · Hiromi Kondo · Kenji Ikeda
Kuniaki Tsuchiya · Rohan de Silva · Andrew Lees
Kenji Kosaka**

Immunohistochemical study of tau accumulation in early stages of Alzheimer-type neurofibrillary lesions

Received: 22 September 2003 / Revised: 20 January 2004 / Accepted: 20 January 2004 / Published online: 16 March 2004

Abstract Accumulation of abnormally phosphorylated tau results in the formation of neurofibrillary tangles (NFTs) in the neuronal cell soma and neuropil threads (NTs) in the cell processes. In the present study, we used immunohistochemistry to investigate serially cut thick tissue sections from the brains of patients with Alzheimer's disease (AD) and non-demented elderly subjects. In the early stages of neurofibrillary pathology, clusters of NTs occurred occasionally in the cerebral cortex. Each NTs cluster, the entire extent of which was observed in the serial sections, corresponded to a dendritic tree that was arborized from a tau-positive neuron. Adult human brain contains six tau isoforms with three having three carboxyl-terminal tandem repeat sequences that are encoded by exon 10 (3R-tau) and the other three having four repeat sequences (4R-tau). Three isoform patterns, 3R-tau(+)/4R-tau(-), 3R-tau(-)/4R-tau(+) and 3R-tau(+)/4R-tau(+), were seen in NFTs in early stage AD lesions. In an individual neuron, the isoform pattern was consistent between the NFTs in the cell soma and the NTs in the cell processes. The results of this study indicate that, in early stages of AD and age-associated neurofibrillary changes, tau accumulates simultaneously in the cell soma and cell processes of affected neurons. The process of AD and age-associated tau pathology is not tau-isoform-specific, but the ratio of 3R-tau and 4R-tau isoforms involved in the neurofibrillary changes varies and is specific to individual neurons.

Keywords Tau · Alzheimer's disease · Neurofibrillary tangle · Neuropil thread

T. Togo · H. Akiyama (✉) · H. Uchikado · H. Kondo · K. Ikeda
Tokyo Institute of Psychiatry,
2-1-8 Kamikitazawa, Setagaya-ku, 156-8585 Tokyo, Japan
Tel.: +81-3-33055701, Fax: +81-3-33298035,
e-mail: akiyama@prit.go.jp

T. Togo · E. Iseki · H. Uchikado · K. Kosaka
Department of Psychiatry,
Yokohama City University School of Medicine, Yokohama, Japan

K. Tsuchiya
Tokyo Metropolitan Matsuzawa Hospital, Tokyo, Japan

R. de Silva · A. Lees
Reta Lila Weston Institute of Neurological Studies,
Royal Free & University College Medical School, London, UK

Introduction

Neurofibrillary lesions constitute a neuropathological hallmark not only in the brain in Alzheimer's disease (AD) but also in the brain during physiological aging not associated with cognitive impairment [15]. They include neurofibrillary tangles (NFTs), which were visualized originally by silver staining and more specifically by tau immunostaining, pretangles, which are defined as non-fibrillar accumulations of tau and are considered to be premature NFTs [3, 4], and neuropil threads (NTs), which account for 85–90% of cortical tau pathology in physiological aging as well as in the early stages of AD [15]. The vast majority of NTs occurs in dendrites, while a small portion of them occurs in axons [17, 22]. The neurofibrillary changes may be central to the neurodegenerative processes in AD. Nevertheless, there has been some controversy with respect to the sequence of tau accumulation in various portions of individual neurons. Some investigators argued that NFTs in the cell soma and NTs in the cell processes were formed simultaneously [4, 5, 7], while others claimed that NTs formation preceded NFTs formation, at least in some neurons [18].

Human tau is encoded by a single gene consisting of 16 exons on chromosome 17q21. Alternative splicing of exons 2, 3 and 10 generates six isoforms that differ by the presence of either three or four carboxyl-terminal tandem repeat sequences that are encoded by exon 10 (3R-tau and 4R-tau, respectively) [1, 12, 16], as well as by the presence or absence of sequences encoded by exons 2 and 3. In some neurodegenerative diseases, 3R-tau or 4R-tau isoforms accumulate differently in a disease-specific manner [2, 9, 10, 20, 21]. On the other hand, both 3R-tau and 4R-tau accumulate in the brain in AD and physiological

aging [12, 19]. There is a paucity of immunohistochemical studies that distinguish between 3R-tau and 4R-tau, since well-characterized antibodies specific to 3R-tau or 4R-tau were only developed recently.

In the present study, we used immunohistochemistry to investigate the early stages of tau accumulation in neurofibrillary lesions in AD and physiological aging. We studied the sequence of tau accumulation in the cell soma and cell processes of individual neurons by analysing the spatial relationship between NFTs/pretangles and NTs in serially cut thick sections. We also describe the tau isoform patterns in the early stages of NFT and NT formation in AD using monoclonal antibodies to 3R-tau and 4R-tau.

Materials and methods

We obtained postmortem brain tissue from 10 autopsied patients: 7 with schizophrenia, 2 with AD and 1 with mild cognitive impairment (MCI). While it remains to be determined whether the neurofibrillary pathology in patients with schizophrenia is comparable to age- and sex-matched controls, evidence indicates that these two groups are indistinguishable by qualitative observations at least [8, 14]. Routine neuropathological examination revealed that all patients had Alzheimer-type pathology (NFTs, NTs and senile plaques). Braak's staging of neurofibrillary changes [6] was stage I in 5 schizophrenia patients; stage II in 2 schizophrenia patients and the MCI patient; stage IV in 1 AD patient and stage VI in the other AD patient. The MCI patient was considered to be a very early stage of AD. Age, sex, diagnosis and Braak stages of every patient are summarized in Table 1. Small brain blocks were taken at the time of autopsy from the hippocampus and the temporal isocortex in the schizophrenia and MCI patients and from the visual cortex and the precentral gyrus in the AD patients so that all brain blocks had early stage Alzheimer-type neurofibrillary pathology.

For immunohistochemistry with a monoclonal mouse antibody to hyperphosphorylated tau, AT8 (Innogenetics, USA), brain blocks were fixed in 4% paraformaldehyde in 0.1 M phosphate buffer, pH 7.4 for 2 days and transferred to a maintenance solution of 15% sucrose in 0.01 M phosphate-buffered saline (PBS), pH 7.4. Serial sections were cut on a freezing microtome at a thickness of 100 µm and stored in the maintenance solution until stained. Six serially cut sections were taken from each patient and stained with AT8. Following a pretreatment with 0.5% H_2O_2 for 30 min, sections were treated for 60 min with 10% bovine serum and incubated for 7 days with AT8 diluted at 0.2 µg/ml in PBS containing 0.3% Triton X-100 (PBS-Tx) and 10% bovine serum. AT8 recognizes tau phosphorylated at serine 199/202. Sections were then treated with a biotinylated anti-mouse IgG antibody (1:1000 in PBS-Tx; Vector Lab, USA) for 24 h, followed by incubation with the avidin-biotinylated horseradish peroxidase (HRP) complex (ABC Elite, Vector Lab) for 3 h. Peroxidase labelling was detected by incubation with a solution containing 0.01% 3,3'-diaminobenzidine (DAB), 0.6% nickel ammonium sulphate, 0.05 M imidazole and 0.00015% H_2O_2. A dark-purple reaction product appeared after about 5 min, at which time the reaction was terminated by transferring the section to PBS-Tx.

For immunohistochemistry with mouse monoclonal anti-3R-tau and anti-4R-tau antibodies (RD3 and RD4, respectively [11, 21]), brain blocks were fixed in 70% ethanol in physiological saline for 2 days and transferred to the maintenance solution. Sections were cut at a thickness of 40 µm. Prior to immunostaining, sections were pretreated with 99% formic acid for 60 s. Sections were incubated for 2 days with RD3 (1:200 in PBS-Tx with 10% bovine serum) or RD4 (1:1000). The primary antibody labelling was visualized similarly to that of AT8. For double immunostaining with RD3 and RD4, sections were first stained with either RD3 or RD4 as described above. Following treatment with 0.5% H_2O_2 for 60 min, the second immunohistochemical cycle for the other antibody was carried out similarly to the first except that nickel ammonium sulphate was eliminated from the DAB solution to yield a brown participate. In this double immunostaining system, the cells labelled brown in the second cycle are considered to be negative for the first cycle primary antibody (1^{st} (-)/2^{nd} (+)). It could not be determined whether the cells labelled purple for the first cycle primary antibody are negative or positive for the second cycle primary antibody (1^{st} (+)/2^{nd} (-) or 1^{st} (+)/2^{nd} (+)) since the dominant purple precipitate may mask the brown precipitate.

Results

Figure 1 illustrates AT8 immunostaining of 100-µm-thick serial sections of the entorhinal cortex from a patient with

Table 1 Data of patients employed in this study (*MCI* mild cognitive impairment, *AD* Alzheimer's disease, *Schizo* schizophrenia, *Hip* hippocampal region including mediobasal temporal isocortex, *Precentral* precentral cortex, *Visual* visual cortex, *Frequency of NFT* + 0–2 per x40 field, ++, 3–5 per x40 field in the area where NFTs are most frequent, *Frequency of NT* + rare, ++ sparse, +++ mild, ++++ moderate, +++++ severe, *NA* not available)

Case no.	Sex, age	Clinical diagnosis	Braak stage	Sample	Frequency		No. of neuritic clusters traced from one end to the other	The proportion of neurons that are DAB+Ni-/Ni+	
					NFT	NT		3R-4R+ / 3R+	3R+4R- / 4R+
1	67M	MCI	2	Hip	+	+	7	NA	NA
2	77M	AD	4	Precentral	+	+	5	NA	NA
				Visual	+	+	7	NA	NA
3	55M	Schizo	1	Hip	++	++	10	NA	NA
4	69F	Schizo	1	Hip	+	+	8	NA	NA
5	72M	Schizo	2	Hip	+	+	3	0.60	0.57
6	50M	Schizo	1	Hip	+	+	1	0.86	0.67
7	65M	Schizo	1	Hip	++	++	1	0.62	0.57
8	85F	Schizo	1	Hip	++	++	4	0.67	0.56
9	76F	Schizo	2	Hip	+	+	6	0.42	0.60
10	75M	AD	6	Precentral	+	+	NA	0.62	0.64
				Visual	+	+	NA	0.72	0.58

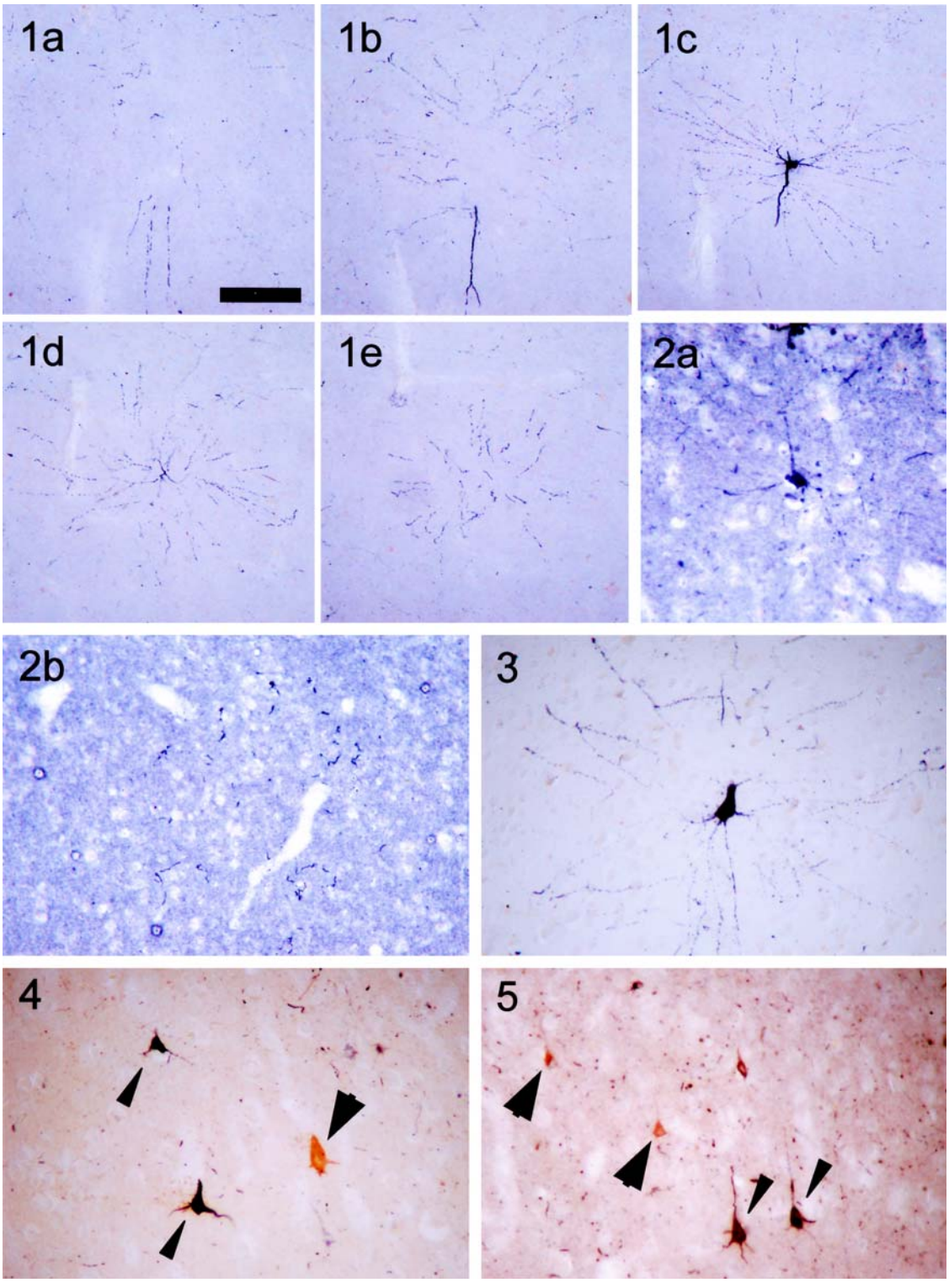

Fig. 1a–e immunostaining of 100-µm-thick, serial sections with AT8, which recognizes abnormally phosphorylated tau. The entorhinal cortex of a patient with schizophrenia, who was stage I of Braak's neurofibrillary pathology staging. A cluster of NTs shows a ring-like or firework-like morphology. Most, if not all, NTs can be traced to the tau-positive neuronal cell body shown in **c**. *Bar*=100 µm

Fig. 2a, b Parahippocampal gyrus of a schizophrenia patient with neurofibrillary pathology (Braak's stage II). The anti-3R-tau antibody (RD3) immunostains neuronal cell soma and proximal processes (**a**) as well as distal processes (**b**). *Bar*=100 µm

Fig. 3 The anti-4R-tau antibody (RD4) immunostains neuronal cell soma, proximal and distal processes. *Bar*=100 µm

Fig. 4 Double immunostaining with RD3 (*purple*) and RD4 (*brown*). The hippocampus of a patient with schizophrenia (Braak's stage I). Two RD3(+) NFTs (*arrowheads*) and an RD3(-)/RD4(+) NFTs (*arrow*) are evident. *Bar*=100 µm

Fig. 5 Double immunostaining with RD4 (*purple*) and RD3 (*brown*). The hippocampus of a patient with schizophrenia (Braak's stage I). RD4(+) NFTs (*arrowheads*) and RD4(-)/RD3(+) NFTs (*arrows*) NFTs are evident. *Bar*=100 µm

schizophrenia. A cluster of NTs, which shows as a firework-like formation, was seen in the neuropil, but NTs were otherwise sparse. In Fig. 1c, most NTs of the cluster seem to be connected with a tau-positive neuron. Since such an observation is possible only in areas in an early stage of neurofibrillary pathology, we employed the mediobasal temporal cortex of patients with Braak's stage I or II and the precentral or visual cortex of patients with AD. The degree of neurofibrillary pathology as well as the number of neuritic clusters traced from one end to the other end are summarized in Table 1. We identified and traced the entire extent of more than 30 independent clusters of NT in the sets of serial sections from all 10 patients. In the center of every cluster that we were able to observe from one end to the other through serial sections, we found a tau-positive neuronal cell soma from which the NT appeared to radiate.

Both 3R-tau and 4R-tau were detected in early stages of AD-type tau pathology. RD3, an anti-3R tau antibody, labelled neuronal cell soma (Fig. 2a) as well as both proximal (Fig. 2a) and distal (Fig. 2b) portions of the cell processes. Figure 3 illustrates a neuron that is stained with RD4, an anti-4R tau antibody. No significant difference was seen between RD3 and RD4 staining with respect to the distribution of immunopositive tau accumulations in the cell soma and processes of individual neurons. Both RD3-positive neurons and RD4-positive neurons were present in all patients examined (Table 1). No difference was found between RD3-positive and RD4-positive neurons with respect to the type of neurons, distribution and morphology.

Double immunostaining with RD3 and RD4 revealed that every patient had RD4-positive and RD3-negative neurons (Fig. 4), as well as RD3-positive and RD4-negative neurons (Fig. 5). In both combinations of double immunostaining, i.e. RD3 first and RD4 second and vice versa, the neurons labelled purple for the first-cycle primary antibody outnumbered the brown-labelled, 1^{st} (-)/2^{nd} (+) neurons. Since purple-labelled, 1^{st} (+) neurons can be either 2^{nd} (-) or 2^{nd} (+), a portion of purple neurons are considered to be positive for both RD3 and RD4. There was no apparent difference in number between RD3(+)/RD4(-) neurons and RD3(-)/RD4(+) neurons. However, it has to be noted that such a comparison was made in nearby, but not identical, sections and that all sections employed in this study contained only a small number of NFT, which may produce some ambiguity.

The hippocampal and temporal regions of the schizophrenia and MCI patients, as well as the precentral and visual cortices of the AD patients, were similar with respect to the occurrence and morphology of RD3 and RD4 immunoreactivity.

Discussion

Accumulation of abnormally phosphorylated tau results in the formation of NFTs in the neuronal cell soma and NTs in the cell processes. In both sites, tau pathology commences as an accumulation of amorphous tau aggregates. Tau aggregates then develop into fibrillar structures that are discerned as paired helical filaments or straight filaments by electron microscopy. It has yet to be established at which cell site, the cell soma or the cell processes, tau abnormality begins in an individual neuron. Braak and colleagues claimed that NFTs in the cell soma and NTs in the cell processes were formed simultaneously [4, 5, 7]. Schmidt et al., on the other hand, argued that more than half of NTs arose from neurons without NFTs [18]. These authors, however, analysed the spatial relationship between NFTs and NTs in single sections.

To overcome this uncertainty, we employed serially cut thick sections, which permitted us to examine every visual field to a depth of 600 μm, so that the entire extent of tau-positive dendritic trees could be observed. We also employed brains with very early stages of Alzheimer-type neurofibrillary pathology where tau-positive neurons were so sparse that we were able to identify a single tau-positive dendritic tree in an area that was essentially devoid of NTs derived from other neurons. With such an experimental design, we traced most, if not all, NTs to their originating neurons. We found that NTs occurred as a cluster in the early stages of neurofibrillary pathology. Each cluster of NTs corresponded to a dendritic tree that was arborized from a single tau-positive neuronal cell body. The results of this study appear to confirm and support the notion by Braak and colleagues. Iwatsubo et al. reported that NTs seemed to grow in both proximal and distal directions in neuronal cell processes [13]. Together with our results, it is suggested that once a tau abnormality is initiated in a given neuron, the process takes place simultaneously in multiple sites of the affected neuron.

Adult human brain contains six tau isoforms, three 3R-tau and three 4R-tau [1, 12, 16]. In neurodegenerative diseases with tau pathology, tau isoforms often accumulate in a disease-specific manner [2, 9, 10, 20, 21]. In AD, biochemical analyses suggest that both 3R-tau and 4R-tau are involved similarly in the disease process. This contrasts with such tauopathies as progressive supranuclear palsy, corticobasal degeneration and argyrophilic grain disease in which 4R-tau predominates and with Pick's disease in which 3R-tau predominates. In the earliest stage of tau abnormality in AD and age-associated neurofibrillary pathology, the isoform pattern of abnormally accumulated tau remains to be elucidated, partly because of the lack of well-characterized antibodies specific for 3R-tau and 4R-tau and applicable to immunohistochemistry.

In the present study, we used two recently developed monoclonal antibodies that are specific to 3R-tau and 4R-tau, respectively [12, 21]. These antibodies work well for immunohistochemistry on postmortem brain tissue sections. We found three isoform patterns of tau in NFTs in the early stage of AD, that is, 3R-tau(+)/4R-tau(-), 3R-tau(-)/4R-tau(+) and 3R-tau(+)/4R-tau(+). All three isoform patterns were found in every patient. While the isoform pattern differed among neurons, it was consistent in all portions of individual neurons. In other words, if the NFTs in a given neuronal cell soma show one isoform pattern, the

NTs in both distal and proximal portions of the cell processes show the same isoform pattern. It is therefore possible to speculate that the process of AD and age-associated tau pathology is not tau-isoform-specific, but that the tau isoforms involved in the pathological processes are specific to each neuron. The tau mRNAs for the six isoforms are not equally expressed in neurons [12]. The isoform pattern of NFTs and NTs might depend on the tau isoforms expressed by the neuron that gives rise to the NFTs and NTs. In this study, we were not able to find significant differences in the distribution and morphology between neurons that accumulate predominantly 3R-tau or 4R-tau.

In summary, we have shown that hyperphosphorylated tau accumulates simultaneously in the cell soma and cell processes in early stages of AD, as well as in age-associated neurofibrillary lesions. The NFTs and NTs in early stages of AD contain either 3R-tau or 4R-tau, or both. Such an isoform difference may depend on the nature of individual neurons that bear the NFT and NT. The pathogenesis of AD and age-associated neurofibrillary changes is not likely to be tau-isoform-specific.

Acknowledgements This study was supported in part by grants-in-aid from the Yokohama Foundation for Advancement of Medical Science as well as a grant from the Ministry of Health, Welfare and Labor of Japan (Brain Science).

References

1. Andreadis A, Brown WM, Kosik KS (1992) Structure and novel exons of the human tau gene. Biochemistry 31:10626–10633
2. Arai T, Ikeda K, Akiyama H, Shikamoto Y, Tsuchiya K, Yagishita S, Beach T, Rogers J, Schwab C, McGeer PL (2001) Distinct isoforms of tau aggregated in neurons and glial cells in brains of patients with Pick's disease, corticobasal degeneration and progressive supranuclear palsy. Acta Neuropathol 101:167–173
3. Bancher C, Brunner C, Lassmann H, Budka H, Jellinger K, Wiche G, Seitelberger F, Grundke-Iqbal I, Iqbal K, Wisniewski HM (1989) Accumulation of abnormally phosphorylated tau precedes the formation of neurofibrillary tangles in Alzheimer's disease. Brain Res 477:90–99
4. Braak E, Braak H, Mandelkow EM (1994) A sequence of cytoskeleton changes related to the formation of neurofibrillary tangles and neuropil threads. Acta Neuropathol 87: 554–567
5. Braak H, Braak E (1988) Neuropil threads occur in dendrites of tangle-bearing nerve cells. Neuropathol Appl Neurobiol 14:39–44
6. Braak H, Braak E (1991) Neuropathological stageing of Alzheimer-related changes. Acta Neuropathol 82:239–259
7. Braak H, Braak E, Grundke-Iqbal I, Iqbal K (1986) Occurrence of neuropil threads in the senile human brain and in Alzheimer's disease: a third location of paired helical filaments outside of neurofibrillary tangles and neuritic plaques. Neurosci Lett 65:351–355
8. Bruton CJ, Crow TJ, Frith CD, Johnstone EC, Owens DG, Roberts GW (1990) Schizophrenia and the brain: a prospective clinico-neuropathological study. Psychol Med 20:285–304
9. Chambers CB, Lee JM, Troncoso JC, Reich S, Muma NA (1999) Overexpression of four-repeat tau mRNA isoforms in progressive supranuclear palsy but not in Alzheimer's disease. Ann Neurol 46:325–332
10. Delacourte A, Sergeant N, Wattez A, Gauvreau D, Robitaille Y (1998) Vulnerable neuronal subsets in Alzheimer's and Pick's disease are distinguished by their tau isoform distribution and phosphorylation. Ann Neurol 43:193–204
11. De Silva R, Lashley T, Gibb G, Hanger D, Hope A, Reid A, Bandopadhyay R, Utton M, Strand C, Jowett T, Khan N, Anderton B, Wood N, Holton J, Revesz T, Lees A (2003) Pathological inclusion bodies in tauopathies contain distinct complements of tau with three or four microtubule-binding repeat domains as demonstrated by new specific monoclonal antibodies. Neuropathol Appl Neurobiol 29:288–302
12. Goedert M, Spillantini MG, Potier MC, Ulrich J, Crowther RA (1989) Cloning and sequencing of the cDNA encoding an isoform of microtubule-associated protein tau containing four tandem repeats: differential expression of tau protein mRNAs in human brain. EMBO J 8:393–399
13. Iwatsubo T, Hasegawa M, Esaki Y, Ihara Y (1992) Lack of ubiquitin immunoreactivities at both ends of neuropil threads. Possible bidirectional growth of neuropil threads. Am J Pathol 140:277–282
14. Jellinger K (1985) Neuromorphological background of pathochemical studies in major psychoses. In: Beckman H (ed) Pathochemical markers in major psychoses. Springer Verlag, Berlin Heidelberg New York, pp 1–23
15. Mitchell TW, Nissanov J, Han LY, Mufson EJ, Schneider JA, Cochran EJ, Bennett DA, Lee VM, Trojanowski JQ, Arnold SE (2000) Novel method to quantify neuropil threads in brains from elders with or without cognitive impairment. J Histochem Cytochem 48:1627–1638
16. Neve RL, Harris P, Kosik KS, Kurnit DM, Donlon TA (1986) Identification of cDNA clones for the human microtubule-associated protein tau and chromosomal localization of the genes for tau and microtubule-associated protein 2. Brain Res 387: 271–280
17. Perry G, Kawai M, Tabaton M, Onorato M, Mulvihill P, Richey P, Morandi A, Connolly JA, Gambetti P (1991) Neuropil threads of Alzheimer's disease show a marked alteration of the normal cytoskeleton. J Neurosci 11:1748–1755
18. Schmidt ML, Murray JM, Trojanowski JQ (1993) Continuity of neuropil threads with tangle-bearing and tangle-free neurons in Alzheimer disease cortex. A confocal laser scanning microscopy study. Mol Chem Neuropathol 18:299–312
19. Sergeant N, David JP, Goedert M, Jakes R, Vermersch P, Buee L, Lefranc D, Wattez A, Delacourte A (1997) Two-dimensional characterization of paired helical filament-tau from Alzheimer's disease: demonstration of an additional 74-kDa component and age-related biochemical modifications. J Neurochem 69:834–844
20. Sergeant N, Wattez A, Delacourte A (1999) Neurofibrillary degeneration in progressive supranuclear palsy and corticobasal degeneration: tau pathologies with exclusively 'exon 10' isoforms. J Neurochem 72:1243–1249
21. Togo T, Sahara N, Yen SH, Cookson N, Ishizawa T, Hutton M, De Silva R, Lees A, Dickson DW (2002) Argyrophilic grain disease is a sporadic 4-repeat tauopathy. J Neuropathol Exp Neurol 61:547–556
22. Yamaguchi H, Nakazato Y, Shoji M, Ihara Y, Hirai S (1990) Ultrastructure of the neuropil threads in the Alzheimer brain: their dendritic origin and accumulation in the senile plaques. Acta Neuropathol 80:368–374